

Electron-Diffraction Study of Gaseous Pentakis(dimethylamido)tantalum(V), Ta(NMe<sub>2</sub>)<sub>5</sub>Kolbjørn Hagen,<sup>1a</sup> Catherine J. Holwill,<sup>1b</sup> David A. Rice,<sup>\*1b</sup> and Jonathan D. Runnacles<sup>1c</sup>

Departments of Chemistry, University of Reading, Whiteknights, Reading RG6 2AD, U.K., University of Trondheim, Trondheim, Norway, and Queen Mary College, University of London, London, U.K.

Received February 12, 1992

The molecular structure of [Ta(NMe<sub>2</sub>)<sub>5</sub>] has been studied by gas-phase electron diffraction. Attempts were made to fit two models, each containing planar C<sub>2</sub>-N-Ta groups, to the experimental data. In model I, the TaN<sub>5</sub> core was given a pyramidal geometry of C<sub>2v</sub> symmetry, while in model II it was assigned a trigonal bipyramidal structure, i.e. D<sub>3h</sub> symmetry. I gave the best fit to the experimental data. From model I the following values were obtained: r<sub>g</sub>(C-H) = 1.120 (10) Å, r<sub>g</sub>(Ta(1)-N(6)) = 1.937 (25) Å [N(6) is on the C<sub>2</sub> axis], r<sub>g</sub>(Ta(1)-N(2)) = 2.040 (6) Å [N(2) is one of the four basal nitrogen atoms], r<sub>g</sub>(C-N) = 1.463 (5) Å, and ∠N(6)-Ta(1)-N(3) = 116.2 (12)°. ∠C-N-C = 110.1 (11)°, ∠N-C-H was held constant at 112.0°, the angles in the base of the C<sub>2v</sub> pyramid were ∠N(2)-Ta(1)-N(3) = 69.4 (31)°, ∠N(2)-Ta(1)-N(5) = 87.8 (36)°, and ∠N(2)-Ta(1)-N(4) = 127.6 (24)°.

## Introduction

We have examined the structures in the gas phase of Zr(NMe<sub>2</sub>)<sub>4</sub><sup>2</sup> and W(NMe<sub>2</sub>)<sub>6</sub><sup>3</sup> and found that the coordination spheres exhibited by the metal atoms in these compounds have T<sub>d</sub> and O<sub>h</sub> symmetry, respectively. The C<sub>2</sub>-N-M (M = Zr, W) fragments in both structures were found to be planar, or very close to planar, and thus the lone pairs of electrons on the nitrogen atoms are available for interaction with vacant orbitals on the metal centers. The occurrence of these interactions is evident from a consideration of the metal to nitrogen distances present in Zr(NMe<sub>2</sub>)<sub>4</sub><sup>2</sup> and W(NMe<sub>2</sub>)<sub>6</sub><sup>3</sup> but this interaction does not cause a detectable deviation of the ZrN<sub>4</sub> and WN<sub>6</sub> coordination spheres from the highest possible symmetry. For the MN<sub>5</sub> cores, which are contained in the compounds M(NMe<sub>2</sub>)<sub>5</sub> (M = Nb, Ta), the two possible regular geometries that have high symmetry are those where the MN<sub>5</sub> fragments have C<sub>4v</sub> or D<sub>3h</sub> symmetry. A single-crystal X-ray study of the niobium compound has been published, and the geometry of the NbN<sub>5</sub> fragment was reported to be "best described as distorted tetragonal bipyramid with the distortions tending towards trigonal bipyramidal".<sup>4</sup> Deviations from ideal symmetry of the type revealed by the study of Nb(NMe<sub>2</sub>)<sub>5</sub> are often ascribed to packing effects, and so we decided to investigate the structure of Ta(NMe<sub>2</sub>)<sub>5</sub> in the gas phase by electron diffraction, thus obtaining the structure free from such influences.

## Experimental Section

**Preparation of Ta(NMe<sub>2</sub>)<sub>5</sub>.** By using a Schlenk tube, Ta(NMe<sub>2</sub>)<sub>5</sub> was prepared by allowing TaCl<sub>5</sub> to react with LiNMe<sub>2</sub> according to published procedures.<sup>5</sup> The product was purified by vacuum sublimation, and spectroscopic and analytical data provided no evidence for the presence of impurities in the sublimed material. Samples (approximately 1.0 g) were sealed under vacuum into glass ampules that could be loaded directly into the Balzers Eldigraph KDG-2 apparatus at the University of Oslo<sup>6,7</sup> and opened in situ. Experiments revealed that no decomposition of the sample took place at the temperature and under the pressure conditions used for the electron-diffraction experiment.

Data were obtained at nozzle-to-plate distances of 497.95 and 248.12 mm with a nozzle temperature of 150 °C. Data from three plates for the longer and four for the shorter nozzle-to-plate distances were used in the final refinements. The data from these two sets of plates cover the ranges 2.25 ≤ s ≤ 14.75 Å<sup>-1</sup> and 6.00 ≤ s ≤ 29.50 Å<sup>-1</sup> (Δs = 0.25 Å<sup>-1</sup>), respectively. The electron wavelength was calibrated using benzene,<sup>8</sup> and the experimental data were processed as described previously<sup>9-13</sup> using published scattering factors.<sup>14,15</sup> Average curves were produced for each camera distance, and these are depicted in Figure 1 together with the theoretical and difference curves for model I, whose definition is given later.

Root mean square amplitudes (*I*) and perpendicular amplitude corrections (*K*) were calculated<sup>16</sup> from an assumed force field using values for the force constants obtained for related molecules. All the longer nonbonded distances have vibrational amplitudes which are strongly dependent upon the force constant assigned to the torsion about the Ta-N bonds. Several different values for this constant were tested, and the best agreement between experiment and theory was obtained with a force constant of 0.30 a J radian<sup>-2</sup>. This value may appear large, but the molecule is very crowded and similar values were used for W(NMe<sub>2</sub>)<sub>6</sub><sup>3</sup> and Zr(NMe<sub>2</sub>)<sub>4</sub>.<sup>2</sup> The importance of obtaining a consistent set of amplitudes was revealed by the study of model II, i.e. the D<sub>3h</sub> model. If the torsional force constants were changed in such a way as to yield vibrational amplitudes in accord with the refined ones, the vibrational amplitudes for the remaining distances assumed values that caused the fit between theory and experiment for model II to be poorer than that shown in Figure 4.

**Analysis of the Structure.** Refinements of the structure were carried out by the least-squares procedure<sup>17</sup> based on intensity curves, by adjusting a theoretical curve to fit the two averaged experimental intensity curves simultaneously, using a unit weight matrix. The theoretical curves used were derived from two models. Each of these models gave a theoretical curve which was defined using a number of variables that were allowed to change during the least-squares refinement. These models were based upon regular TaN<sub>5</sub> cores. In model I the TaN<sub>5</sub> core was assigned C<sub>2v</sub> symmetry, while in model II it was given D<sub>3h</sub> symmetry. Model I is depicted in Figure 2, which also contains the atom-numbering scheme. This model was refined using the following variables: r(C-H), r(Ta-N) [where r(Ta-N) = 0.5{r(Ta(1)-N(6)) + {r(Ta(1)-N(2))}}, Δr(Ta-N)

(8) Tamagawa, K.; Iijima, T.; Kimura, M. *J. Mol. Struct.* 1976, 30, 243.(9) Hagen, K.; Hedberg, K. *J. Am. Chem. Soc.* 1973, 95, 1003.(10) Gundersen, G.; Hedberg, K. *J. Chem. Phys.* 1969, 51, 2500.(11) Andersen, B.; Seip, H. M.; Strand, T. G.; Stølevik, R. *Acta Chem. Scand.* 1969, 23, 3224.

(12) Hedberg, L. Abstracts of the 5th Austin Symposium on Gas-Phase Molecular Structure. Austin, TX, March 1974, p 37.

(13) Hagen, K.; Hobson, R. J.; Rice, D. A.; Turp, N. *J. Mol. Struct.* 1985, 128, 33.(14) Schäfer, L.; Yates, A. C.; Bonham, R. A. *J. Chem. Phys.* 1971, 56, 3056.(15) Cromer, D. T. *J. Chem. Phys.* 1969, 50, 4857.(16) Hilderbrandt, R. L.; Weiser, J. D. *J. Chem. Phys.* 1971, 55, 4648.(17) Hedberg, K.; Iwasaki, M. *Acta Crystallogr.* 1964, 17, 529.

(1) (a) University of Trondheim. (b) University of Reading. (c) Queen Mary College, University of London.

(2) Hagen, K.; Holwill, C. J.; Rice, D. A.; Runnacles, J. D. *Inorg. Chem.* 1988, 27, 2032.(3) Hagen, K.; Holwill, C. J.; Rice, D. A.; Runnacles, J. D. *Acta Chem. Scand.* 1988, Ser. A42, 578.(4) Heath, C.; Hursthouse, M. B. *Chem. Commun.* 1971, 143.(5) Bradley, D. C.; Thomas, I. M. *Can. J. Chem.* 1962, 40, 1355.(6) Ziel, W.; Haase, J.; Wegmann, L. *Z. Instrumentenk.* 1966, 74, 84.(7) Bastiansen, O.; Graber, G.; Wegmann, L. *Balzers High Vacuum Rep.* 1969, 25, 1.

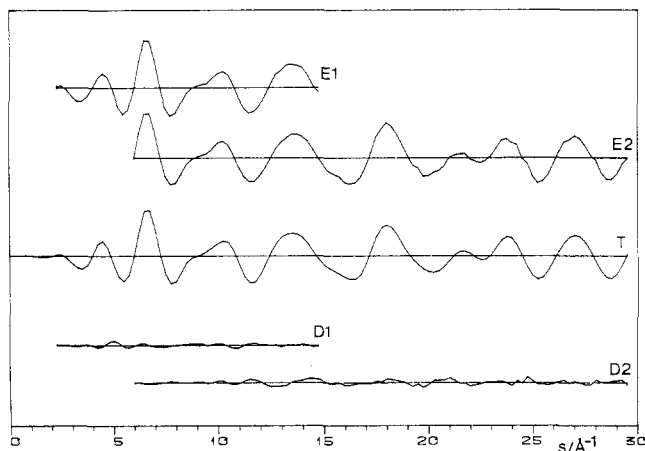


**Figure 1.** Intensity curves  $s[I_m(s)]$  for  $\text{Ta}(\text{NMe}_2)_5$ . The experimental curves are averages of all plates for the two camera distances. The theoretical curve was calculated from the structural parameters shown in Table Ia. The difference curves result from subtracting the relevant part of the theoretical curve from the experimental curves.

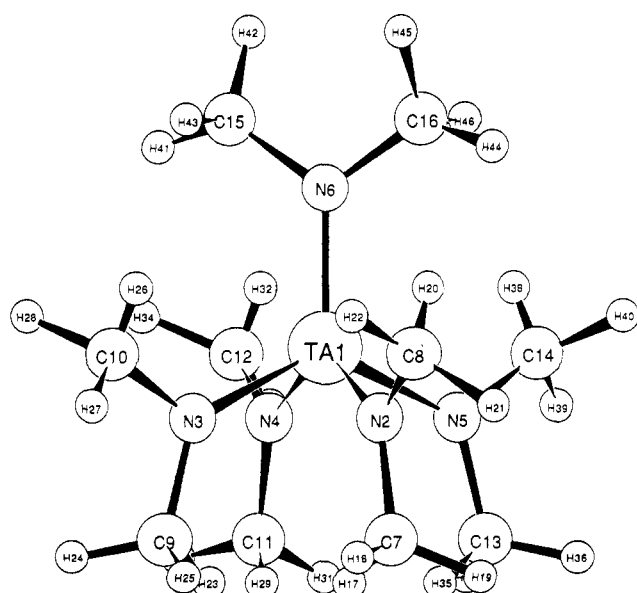


**Figure 2.** Molecular picture for model I with the atom-numbering scheme.

[where  $\Delta r(\text{Ta}-\text{N}) = \{r(\text{Ta}(1)-\text{N}(6)) - r(\text{Ta}(1)-\text{N}(2))\}$ ,  $r(\text{C}-\text{N})$ ,  $\angle \text{N}(6)-\text{Ta}-\text{N}(2)$ ,  $\angle \text{C}(15)-\text{N}(6)-\text{C}(16)$ ,  $\angle \text{N}(6)-\text{C}(15)-\text{H}(42)$ ,  $\angle \Phi$  [which is the angle between the projections formed by  $\text{N}(2)-\text{Ta}$  and  $\text{N}(3)-\text{Ta}$  on the plane through  $\text{Ta}(1)$  that is orthogonal to  $\text{N}(6)-\text{Ta}(1)$ ], and the torsion angle  $\angle \text{N}(6)-\text{Ta}(1)-\text{N}(3)-\text{C}(9)$ . In the refinement of model I, the following conditions were applied: 1. All the  $\text{C}_2-\text{N}-\text{Ta}$  fragments were assumed to be planar.<sup>2,3</sup> In initial investigations, in which the  $\text{C}_2-\text{N}-\text{Ta}$  planes were allowed to deviate from planarity, no significant improvement in the fit between the experimental and theoretical data was observed. 2. The methyl groups were assumed to have  $\text{C}_{3v}$  symmetry with the  $\text{C}_3$  axis being along the  $\text{C}-\text{N}$  bonds. 3. The plane formed by  $\text{C}(15)$ ,  $\text{N}(6)$ ,  $\text{C}(16)$ , and  $\text{Ta}(1)$  was aligned to bisect  $\angle \text{N}(3)-\text{Ta}(1)-\text{N}(4)$  and  $\angle \text{N}(2)-\text{Ta}(1)-\text{N}(5)$ . Refinements in which the torsion angle  $\text{N}(2)-\text{Ta}(1)-\text{N}(6)-\text{C}(15)$  was allowed to vary were not significantly better than those in which the angle was fixed. The results of the final refinement, using this model, are shown in Table Ia.

Model II (see Figure 3 where the atom-numbering scheme is given), which has a  $\text{D}_{3h}$  core, was defined using the variables  $r(\text{Ta}(1)-\text{N}(2))$ ,  $r(\text{Ta}(1)-\text{N}(4))$ ,  $r(\text{C}-\text{N})$ ,  $r(\text{C}-\text{H})$ ,  $\angle \text{C}-\text{N}-\text{C}$ , and  $\angle \text{N}-\text{C}-\text{H}$ . In addition to the bond distances and valence angles, a torsion angle,  $\angle \text{C}(11)-\text{N}(4)-\text{Ta}(1)-\text{N}(2)$ , allowing rotation about  $\text{Ta}(1)-\text{N}(X)$  ( $X = 4-6$ ) was included. The angle was defined so that rotation about all three  $\text{Ta}-\text{N}$  bonds was equivalent. Conditions 1 and 2 used for model I were employed with model II. A further assumption was made, namely, that  $\text{N}(2)$ ,  $\text{C}(7)$ ,  $\text{C}(8)$ ,  $\text{Ta}(1)$ ,  $\text{N}(3)$ ,  $\text{C}(9)$ , and  $\text{C}(10)$  form a plane which is at  $90^\circ$  to  $\text{Ta}(1)-\text{N}(4)$ . Refinements with the plane formed by  $\text{N}(2)$ ,  $\text{C}(7)$ , and

**Table I.** Final Structural Parameters for  $\text{Ta}(\text{NMe}_2)_5$  from Model I, in Which  $\text{TaN}_5$  Has  $\text{C}_{2v}$  Symmetry, and from Model II, in Which  $\text{TaN}_5$  Has  $\text{D}_{3h}$  Symmetry<sup>a</sup>

(a) Model I			
variable params	$r_g$	$l_{\text{calc}}$	
$r(\text{Ta}-\text{N})^a$	1.983 (15)		
$\Delta(\text{Ta}-\text{N})^a$	-0.052 (10)		
$r(\text{C}-\text{H})$	1.120 (10)	0.079 [0.068 (10)] <sup>b</sup>	
$r(\text{C}-\text{N})$	1.463 (5)	0.050 [0.053 (6)] <sup>b</sup>	
$\angle \text{N}(6)-\text{Ta}(1)-\text{N}(2)$	116.2 (12)		
$\angle \text{C}-\text{N}-\text{C}$	110.1 (11)		
$\angle \Phi^c$	78.8 (39)		
$\angle \text{N}(6)-\text{Ta}(1)-\text{N}(3)-\text{C}(9)$	169 (27)		
$\angle \text{N}-\text{C}-\text{H}$	112.0 <sup>d</sup>		
dependent params	$r_g$	$l_{\text{calc}}$	
$r(\text{Ta}(1)-\text{N}(6))$	1.937 (25)	0.050	
$r(\text{Ta}(1)-\text{N}(2))$	2.040 (6)	0.050	
$\angle \text{N}(2)-\text{Ta}(1)-\text{N}(3)$	69.4 (31)		
$\angle \text{N}(2)-\text{Ta}(1)-\text{N}(5)$	87.8 (36)		
$\angle \text{N}(2)-\text{Ta}(1)-\text{N}(4)$	127.6 (24)		
$r(\text{N}(2)\cdots\text{N}(6))$	3.372 (19)	0.093	
$r(\text{N}(2)\cdots\text{N}(3))$	2.324 (93)	0.131	
$r(\text{N}(2)\cdots\text{N}(4))$	3.656 (28)	0.087	
$r(\text{N}(2)\cdots\text{N}(5))$	2.827 (91)	0.118	
$r(\text{C}(7)\cdots\text{C}(8))$	2.386 (18)	0.089	
$r(\text{Ta}(1)\cdots\text{C}(15))$	3.012 (12)	0.088	
$r(\text{Ta}(1)\cdots\text{C}(7))$	3.106 (8)	0.089	
short camera		long camera	
$R$ values <sup>e</sup>		0.127      0.088	
(b) Model II			
variable params	$r_g$	$l_{\text{refined}}$	$l_{\text{calc}}$
$r(\text{Ta}(1)-\text{N}(6))$	2.054 (26)	0.062 (7) <sup>f</sup>	0.051
$r(\text{Ta}(1)-\text{N}(2))$	2.014 (15)	0.061 (7) <sup>f</sup>	0.050
$r(\text{C}-\text{H})$	1.119 (13)	0.079	0.079
$r(\text{C}-\text{N})$	1.464 (6)	0.054 (6)	0.050
$\angle \text{Ta}(1)-\text{N}-\text{C}$	123.9 (9)		
$\angle \text{C}(11)-\text{N}(4)-\text{Ta}(1)-\text{N}(2)$	162 (4)		
$\angle \text{N}-\text{C}-\text{H}$	114.0 <sup>d</sup>		
dependent params	$r_g$	$l_{\text{refined}}$	$l_{\text{calc}}$
$r(\text{N}(2)\cdots\text{N}(4))$	2.875 (11)	0.131 (32) <sup>g</sup>	0.117
$r(\text{N}(2)\cdots\text{N}(3))$	4.100 (35)	0.085 (21) <sup>g</sup>	0.071
$r(\text{N}(4)\cdots\text{N}(5))$	3.479 (18)	0.114 (22) <sup>g</sup>	0.100
$r(\text{C}(9)\cdots\text{C}(10))$	2.433 (25)	not refined	0.091
$r(\text{Ta}(1)\cdots\text{C}(7))$	3.121 (16)	0.114 (8) <sup>h</sup>	0.090
$r(\text{Ta}(1)\cdots\text{C}(11))$	3.086 (15)	0.114 (8) <sup>h</sup>	0.090
$\angle \text{C}(11)-\text{N}(4)-\text{Ta}(1)-\text{N}(6)$	29 (8)		
short camera		long camera	
$R$ values <sup>e</sup>		0.146      0.140	

<sup>a</sup> Atom-numbering schemes for models I and II are found in Figures 2 and 3. Distances and amplitudes are in Å, and angles are in deg. Uncertainties are  $2\sigma$  plus an estimate for errors in the wavelength, etc. The distance  $r(\text{Ta}-\text{N}) = 0.5\{r(\text{Ta}(1)-\text{N}(6)) + r(\text{Ta}(1)-\text{N}(2))\}$ , while  $\Delta r(\text{Ta}-\text{N}) = \{r(\text{Ta}(1)-\text{N}(6)) - r(\text{Ta}(1)-\text{N}(2))\}$ . <sup>b</sup> These are the only two amplitudes that were refined. <sup>c</sup>  $\angle \Phi$  is the angle between the projections of  $\text{N}(2)-\text{Ta}$  and  $\text{N}(3)-\text{Ta}$  onto the plane through  $\text{Ta}(1)$  that is orthogonal to  $\text{N}(6)-\text{Ta}(1)$ . <sup>d</sup> This angle was refined to  $112.0^\circ$  (model I) or  $114.0^\circ$  (model II) by having all the other variables held at the values shown above. <sup>e</sup>  $R = [\sum w_i \Delta_i^2 / \sum w_i (s_i I_i(\text{obsd}))^2]^{1/2}$ , where  $\Delta_i = s_i I_i(\text{obsd}) - s_i I_i(\text{calc})$ . <sup>f</sup> Amplitudes refined as a group. <sup>g</sup> Amplitudes refined as a group. <sup>h</sup> Amplitudes refined as a group.

$\text{C}(8)$  orthogonal to the plane formed by  $\text{N}(3)$ ,  $\text{C}(9)$ , and  $\text{C}(10)$  did not converge, and when  $\text{Ta}-\text{N}(2)$  and  $\text{Ta}-\text{N}(3)$  torsion angles were allowed to refine independently, no further improvement in the fit to the experimental data could be obtained. The results of the final refinement using this model are shown in Table Ib.

The radial distribution curves for both models were calculated in the usual way using the values for the parameters given in Table Ia,b. The experimental curve and the difference curves between the experimental and theoretical curves are shown in Figure 4. The correlation matrix for the final refinement for model I is given in Table II.

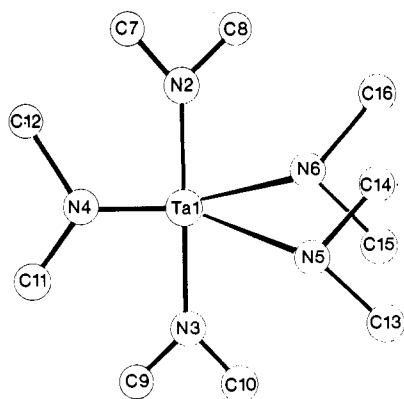


Figure 3. Molecular picture of the TaN<sub>5</sub> core for model II.

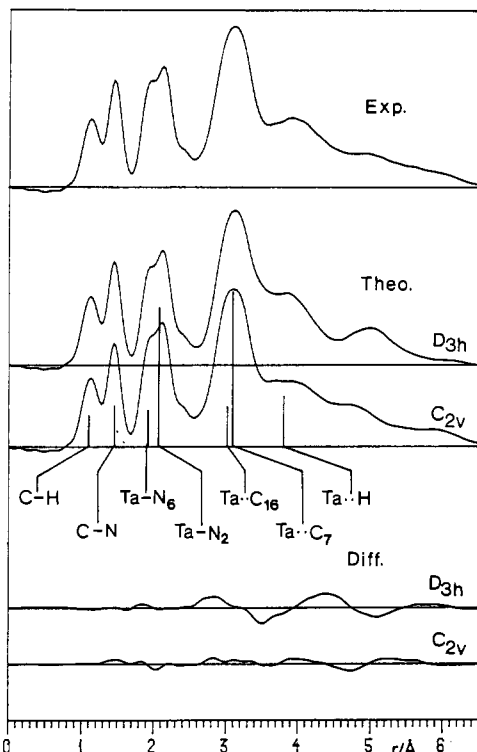


Figure 4. Radial distribution curves for models I and II, showing the experimental radial distribution curve, and the difference curves obtained by subtracting the theoretical radial distribution curves (calculated from the data given in Table Ia,b) from the experimental radial distribution curve shown here. The radial distribution curves were calculated from the curves in Figure 1 after multiplication by  $(Z_{\text{Ta}}Z_{\text{N}}/f_{\text{Ta}}f_{\text{N}}) \exp(-0.0025s^2)$  and using theoretical data for the unobserved area  $s < 2.25 \text{ \AA}^{-1}$ . The contributions of the most important distances are indicated on the radial distribution curves as bars, and the heights of the bars are proportional to the weights of the distances.

## Results and Discussion

As stated in the Introduction, for the TaN<sub>5</sub> core on Ta(NMe<sub>2</sub>)<sub>5</sub> there are two possible regular geometries; one has  $D_{3h}$  symmetry, while the other has  $C_{4v}$ . However, the presence of the methyl groups that are bonded to the nitrogen atoms reduces the overall symmetry even if the presence of the hydrogen atoms is ignored. For the model based upon the idealized regular  $C_{4v}$  TaN<sub>5</sub> core, model I, the highest possible overall symmetry becomes  $C_{2v}$ . Indeed during refinement of model I the TaN<sub>5</sub> fragment refined to one having  $C_{2v}$  symmetry. The highest overall symmetry of  $C_{2v}$  is obtained by the torsion angle between the basal N-C bonds [e.g. N(2)-C(7); see Figure 2 for atom-numbering scheme] and the axial Ta-N bond [Ta(1)-N(6)] being 180° and the plane formed by C(15), N(6), and C(16) bisecting  $\angle$ N(3)-Ta(1)-N(4) and  $\angle$ N(2)-Ta(1)-N(5). For the model based upon a  $D_{3h}$  core, model

II, the situation is more complex (Figure 3). The most symmetrical arrangement is with C(7), C(8), N(2), Ta(1), N(3), C(10), and C(9) forming a plane and with C(11)...C(12), C(13)...C(14), and C(15)...C(16) forming a torsion angle of 0° with Ta(1)-N(2). Even so this gives rise to a 6-fold rotation barrier and the barriers to such rotations are known to be very small as in methylbenzene.

Attempts were made to fit both models to the experimental data. The results for the final refinements are contained in Table Ia (model I) and Table Ib (model II). From the Table Ia,b it can be seen that lower  $R$  factors are obtained with model I. Model I is using a larger number of parameters than model II. Thus, it could be argued that it is the greater number of variables associated with model I, rather than the correctness of the model, that leads to the lowest  $R$  factor. However, the  $R$  values obtained with model I, and the fit between the theoretical and experimental radial distribution curves (Figure 4), are so much better with model I than model II that we believe model I is the correct one. It should be noted, however, that Ta(NMe<sub>2</sub>)<sub>5</sub> is a very complicated molecule to study by gas-phase electron diffraction and the final results will depend on the choice of model. We have investigated many models and present here an investigation into what we believe are the two most likely ones.

The Ta-N distances obtained from model I are  $r(\text{Ta}(1)-\text{N}(6)) = 1.937(25) \text{ \AA}$  and  $r(\text{Ta}(1)-\text{N}(2)) = 2.040(6) \text{ \AA}$ , with the bond along the  $C_2$  axis being significantly shorter than the bonds to the base of the  $C_{2v}$  pyramid. These distances are similar to the related distances found in  $\text{W}(\text{NMe}_2)_6$  [ $r_g(\text{W}-\text{N}) = 2.035(5) \text{ \AA}$ ]<sup>3</sup> and  $\text{Zr}(\text{NMe}_2)_4$  [ $r_g = 2.032(25) \text{ \AA}$ ].<sup>2</sup> The difference in bond lengths between the two types of Ta-N bond is not ascribable to the influence of nonbonding interactions. From a consideration of Ta(1)-N(6) and Ta(1)-N(2) distances and the sizes of the various N-Ta-N angles (Table Ia), it is clear that the nonbonded interactions formed by the C(15)C(16)N(6) group with C(8), C(10), C(11), and C(12) are considerably longer than the shortest interactions between the rest of the  $C_2\text{N}$  groups. This statement would be true even if  $r(\text{Ta}(1)-\text{N}(6))$  were equal to  $r(\text{Ta}(1)-\text{N}(2))$ . Thus, the difference observed between  $r(\text{Ta}(1)-\text{N}(6))$  and  $r(\text{Ta}(1)-\text{N}(2))$  is attributable to the Ta(1)-N(6) bond being of a higher order than Ta(1)-N(2). The molecule Ta(NMe<sub>2</sub>)<sub>5</sub> is a twenty-electron one with five electrons being provided by the metal center plus three further electrons from each of the NMe<sub>2</sub> fragments. As the maximum number of bonding molecular orbitals that can be formed by the metal is nine, there must be at least two electrons in an antibonding or nonbonding orbital. As all the C-N-C groups were found to be planar, each nitrogen atom can be considered to contribute a  $\sigma$  orbital and p orbital to the bonding of the TaN<sub>5</sub> moiety. Under  $C_{2v}$  symmetry, and with C(15)N(6)C(16) in the  $zx$  plane, the orbitals provided by N(6) are of  $A_1[\sigma]$  and  $B_2[p]$  symmetry. The  $\sigma$  orbitals from the remaining four nitrogen atoms combine to give four symmetry combinations that span  $A_1$ ,  $A_2$ ,  $B_1$ , and  $B_2$ . A further four combinations, which also span  $A_1$ ,  $A_2$ ,  $B_1$ , and  $B_2$ , are derived from the four p orbitals (one from each of the four symmetry-related nitrogen atoms). The atomic orbitals of the metal have the following symmetry under  $C_{2v}$ :  $A_1$ , 6s, 6p<sub>z</sub>, and 5d<sub>z<sup>2</sup></sub>;  $A_2$ , 5d<sub>xy</sub>;  $B_1$ , 5d<sub>xz</sub> and 6p<sub>x</sub>;  $B_2$ , 5d<sub>yz</sub> and 6p<sub>y</sub>.

Thus, it is clear that one of the two  $A_2$  orbitals, formed by the four symmetry-related nitrogen atoms, must be nonbonding as only one of the metal orbitals has  $A_2$  symmetry. There are three symmetry combinations from the orbitals of the nitrogen atoms that are of  $B_2$  symmetry but only two metal orbitals of this symmetry. Furthermore, from a priori considerations, the p orbital from N(6)[ $B_2$ ] would be expected to overlap quite efficiently with 5d<sub>yz</sub> and 6p<sub>y</sub>. Thus, one of the  $B_2$  symmetry combinations arising from the orbitals of the four symmetry-related nitrogen atoms is expected to be nonbonding. These observations are in accord with Ta(1)-N(6) being of higher bond order than

**Table II.** Correlation Matrix ( $\times 100$ ) for the Final Refinement of Model I

param	$\sigma^a$	$r_1$	$r_2$	$r_3$	$\angle_4$	$\angle_5$	$\angle_6$	$\angle_7$	$r_8$	$l_9$	$l_{10}$	$l_{11}$	$l_{12}$
$r(\text{Ta}-\text{N})^b$	0.366	100	-11	-15	-19	-34	27	16	-95	-27	-41	-6	-18
$r(\text{C}-\text{N})$	0.11		100	10	10	4	-1	-11	4	-2	-1	8	-9
$r(\text{C}-\text{H})$	0.24			100	8	2	6	17	16	7	19	6	0
$\angle \text{N}(6)-\text{Ta}(1)-\text{N}(2)$	40.5				100	-37	-18	29	21	11	22	37	-28
$\angle \text{C}-\text{N}-\text{C}$	37.0					100	1	9	-27	-6	-13	-35	36
$\angle \Phi^c$	129.0						100	-25	26	15	21	-43	32
$\angle \text{N}(6)-\text{Ta}(1)-\text{N}(3)-\text{C}(9)$	912							100	-9	11	23	12	-18
$\Delta(\text{Ta}-\text{N})^b$	2.49								100	31	44	7	18
$l(\text{C}-\text{H})$	0.24									100	42	8	7
$l(\text{C}(16)-\text{N}(6))$	0.16										100	16	8
$l(\text{C}\cdots\text{N})^d$	3.32											100	-62
$l(\text{Ta}\cdots\text{H})^e$	3.87												100

<sup>a</sup> Standard deviations ( $\times 100$ ) from least squares. Distances and amplitudes are in Å and angles are in deg. <sup>b</sup> The distance  $r(\text{Ta}-\text{N}) = 0.5\{r(\text{Ta}(1)-\text{N}(6)) + r(\text{Ta}(1)-\text{N}(2))\}$ , while  $\Delta r(\text{Ta}-\text{N}) = \{r(\text{Ta}(1)-\text{N}(6)) - r(\text{Ta}(1)-\text{N}(2))\}$ . <sup>c</sup>  $\angle \Phi$  is the angle between the projections of  $\text{N}(2)-\text{Ta}$  and  $\text{N}(3)-\text{Ta}$  onto the plane through  $\text{Ta}(1)$  that is orthogonal to  $\text{N}(6)-\text{Ta}(1)$ . <sup>d</sup> All nonbonded  $\text{C}\cdots\text{N}$  amplitudes refined as a group. <sup>e</sup> All  $\text{Ta}\cdots\text{H}$  amplitudes refined as a group.

the other Ta-N bonds and  $r(\text{Ta}(1)-\text{N}(6))$  being smaller than  $r(\text{Ta}(1)-\text{N}(2))$ .

The multiple nature of the  $\text{Ta}(1)-\text{N}(6)$  bond is further supported by the size of the  $\angle \text{N}(6)-\text{Ta}(1)-\text{N}(2)$  angle [ $116.2$  ( $12^\circ$ )]. It has been found for a whole range of compounds of the type  $\text{MYX}_4$  (where  $\text{M} = \text{Mo}, \text{W}, \text{Os}, \text{or Re}$ ,  $\text{X} = \text{F}, \text{Cl}, \text{or Br}$ , and  $\text{Y} = \text{O}, \text{S}, \text{or Se}$ ) that  $\angle \text{Y}-\text{M}-\text{X} = 102.4$  ( $13$ )- $105.5$  ( $15$ ) $^\circ$ ,<sup>18</sup> and this observation has been attributed to the influence of the  $\text{Y}-\text{M}$  multiple bonds. However, in the present molecule the two methyl groups bound to  $\text{N}(6)$  will cause steric interactions that are likely to influence the size of  $\angle \text{N}(6)-\text{Ta}(1)-\text{N}(2)$ .

The strong deviation of the  $\text{TaN}_5$  fragment from  $C_{4v}$  symmetry is caused by the influence of the presence of the  $\text{C}(15)-\text{N}(6)-\text{C}(16)$  group and the multiple bond  $\text{Ta}-\text{N}(6)$ , which lead to nonbonded  $\text{N}\cdots\text{N}$  distances of  $2.324$  ( $93$ ) Å ( $\text{N}(2)\cdots\text{N}(3)$ ) and  $2.827$  ( $91$ ) Å ( $\text{N}(2)\cdots\text{N}(4)$ ). The former distance seems quite short for a nonbonded distance, but there have been no gas-phase structural determinations where comparable  $\text{N}\cdots\text{N}$  distances could be expected, that is for compounds where the coordination sphere is irregular and of the type  $\text{MN}_n$  ( $n \geq 4$ ). However, short  $\text{F}\cdots\text{F}$  distances are common; for example, in  $\text{PH}_2\text{F}_3$  there is an  $\text{F}\cdots\text{F}$  distance of  $2.235$  ( $2$ ) Å.<sup>19</sup>

There have been few structural investigations by gas-phase electron diffraction of  $\text{MX}_5$  species, where  $\text{M}$  is a transition element. The most recent report of a definitive nature concerns  $\text{VF}_5$ ,<sup>20</sup> for which two models were studied. In one model  $D_{3h}$

symmetry was assumed, while in the other all the V-F bonds were allowed to vary independently. Although the best fit was obtained with the model having the most variables, the difference between the results from the two models was said not to be statistically significant. In contrast, we believe model I, based upon a  $C_{2v}$  core, to be the better one for  $\text{Ta}(\text{NMe}_2)_5$ . The difference we attribute to the influence of the lone pair electrons on the nitrogen atoms. Although F is isolobal with  $\text{Me}_2-\text{N}^+$  (or alternatively  $\text{F}^-$  is isolobal with  $\text{Me}_2-\text{N}^-$ ), donation of a lone pair in a p orbital is a more facile process for the nitrogen-containing system than for fluorine. Further evidence for model I being the correct one was obtained during the least-squares refinements of model II. A modification was introduced to allow the  $\text{N}-\text{Ta}-\text{N}$  bond angles to vary independently. These alterations led to refinements where a  $\text{TaN}_5$  core with close to  $C_{2v}$  symmetry was obtained but the  $R$  factor obtained was not as low as that obtained with model I.

**Acknowledgment.** We thank the SERC for awards to C.J.H. and J.D.R. Special thanks are due to Mr. Hans Volden and Ms. Snefrid Gundersen for their help in collection and primary manipulation of the electron-diffraction data and to the Norwegian Research Council for Science and the Humanities for their financial support of K.H. and the provision of the electron-diffraction facilities at The University of Oslo. NATO is thanked for the award of a travel grant (No. 117/82).

(18) Page, E. M.; Rice, D. A.; Hagen, K.; Hedberg, L.; Hedberg, K. *Inorg. Chem.* **1991**, *30*, 4758.

(19) Downs, A. J.; McGrady, G. S.; Barnfield, E. A.; Rankin, D. W. H. *J. Chem. Soc., Dalton Trans.* **1989**, 545.

(20) Hagen, K.; Gilbert, M. M.; Hedberg, L.; Hedberg, K. *Inorg. Chem.* **1982**, *21*, 2690.